

## Colossal Magnetoresistance by Avoiding a Ferromagnetic State in the Mott System $\text{Ca}_3\text{Ru}_2\text{O}_7$

X. N. Lin,<sup>1</sup> Z. X. Zhou,<sup>2</sup> V. Durairaj,<sup>1</sup> P. Schlottmann,<sup>2</sup> and G. Cao<sup>1,\*</sup>

<sup>1</sup>*Department of Physics and Astronomy, University of Kentucky, Lexington, Kentucky 40506, USA*

<sup>2</sup>*National High Magnetic Field Laboratory, Florida State University, Tallahassee, Florida 32310, USA*

(Received 2 February 2005; published 30 June 2005)

Transport and magnetic studies of  $\text{Ca}_3\text{Ru}_2\text{O}_7$  for temperatures ranging from 0.4 to 56 K and magnetic fields  $B$  up to 45 T lead to strikingly different behavior when the field is applied along the different crystal axes. A ferromagnetic (FM) state with full spin polarization is achieved for the  $B \parallel a$  axis, but colossal magnetoresistance is realized *only* for the  $B \parallel b$  axis. For the  $B \parallel c$  axis, Shubnikov–de Haas oscillations are observed and followed by a less resistive state than that for  $B \parallel a$ . Hence, in contrast with standard colossal magnetoresistive materials, the FM phase is the *least favorable* for electron hopping. These properties together with highly unusual spin-charge-lattice coupling near the Mott transition (48 K) are driven by the orbital degrees of freedom.

DOI: 10.1103/PhysRevLett.95.017203

PACS numbers: 75.47.Gk, 71.30.+h, 75.30.Kz

In ruthenates, in particular, the bilayered  $\text{Ca}_3\text{Ru}_2\text{O}_7$ , the orbital degrees of freedom play an important role prompting novel phenomena through the coupling of the orbits to the spin (spin-orbit interaction) and to the lattice (Jahn-Teller effect). The extension of the  $4d$  orbitals leads to comparable and thus competing energies for the crystalline fields, Hund's rule interactions, spin-orbit coupling,  $p$ - $d$  hybridization, and electron-lattice coupling. Physical properties are then particularly susceptible to small perturbations by external magnetic fields and slight structural changes. Colossal magnetoresistance (CMR) normally occurs for the field applied along the easy axis of magnetization. In this Letter, we present evidence for an unusual CMR in  $\text{Ca}_3\text{Ru}_2\text{O}_7$  realized *only* when  $B$  is *perpendicular* to the easy axis of magnetization ( $a$  axis) or when the spin-polarized state is avoided. This CMR phenomenon is fundamentally different from those of all other magnetoresistive systems, which are primarily driven by spin polarization. In addition, for the  $B \parallel c$  axis, Shubnikov–de Haas oscillations are observed and followed by a much more conducting state than that for  $B \parallel a$ . The results in this Letter include the resistivity for the current along the  $c$  axis,  $\rho_c$ , and along the  $a$  axis,  $\rho_a$ , taken in  $B$  up to 45 T at 0.4 K and the field dependence of the magnetization  $M$  and  $\rho_c$  in the vicinity of  $T_{\text{MI}}$  ( $40 \leq T < 56$  K) for  $B$  applied along the  $a$ ,  $b$ , and  $c$  axes. All results provide a coherent picture illustrating that the spin-polarized state is energetically the *least favorable* for electron hopping, and that orbital order and its coupling to lattice and spin degrees of freedom drive the exotic electronic and magnetic properties of  $\text{Ca}_3\text{Ru}_2\text{O}_7$ .

In the ruthenates with  $\text{Ru}^{4+}$  ( $4d^4$ ) ions, the Hund's rule energy maximizing the total spin at each Ru site is not large enough to overcome the  $e_g$ - $t_{2g}$  crystalline field splitting, so that the  $e_g$  levels are not populated. Hence, one  $t_{2g}$  orbital is doubly occupied, while the other two host a single electron each. The three  $t_{2g}$  levels ( $d_{xy}$ ,  $d_{zx}$ , and  $d_{yz}$ ) are expected to have different energies because the  $\text{RuO}_6$

octahedra are deformed (all lattice parameters are different). These splittings are larger than the thermal energy  $k_B T$  and the Zeeman effect. The octahedra are corner shared and often tilted. The tilting plays an important role in the overlap between orbitals of neighboring octahedra. Small changes in the tilting can result in qualitative changes in the properties. Local density approximation calculations for  $\text{Sr}_3\text{Ru}_2\text{O}_7$ , which shares common aspects with  $\text{Ca}_3\text{Ru}_2\text{O}_7$ , find the Fermi surface very sensitive to small structural changes which readily shift the Fermi energy [1]. In view of the strong sensitivity to crystalline field and tilting angle asymmetries, the coupling of the magnetic field to the system depends on the orientation of the field. Consequently, different properties can be expected if the magnetic field is applied along the different crystallographic axes.

The Mott transition in the single-layered  $\text{Ca}_{2-x}\text{Sr}_x\text{RuO}_4$  has been attributed theoretically [2–5] and experimentally [6,7] to Coulomb interactions and orbital ordering (OO). The wealth of experimental results for the bilayered  $\text{Ca}_3\text{Ru}_2\text{O}_7$  still needs interpretation, but its origin is likely to be OO [8–19]. The crystal structure of  $\text{Ca}_3\text{Ru}_2\text{O}_7$  is severely distorted by a tilt of the  $\text{RuO}_6$  octahedra [9], which projects primarily onto the  $ac$  plane ( $153.22^\circ$ ), while it only slightly affects the  $bc$  plane ( $172.0^\circ$ ) [9]. These crucial bond angles directly impact the band structure and are the origin of the anisotropic properties of the compound. In zero field,  $\text{Ca}_3\text{Ru}_2\text{O}_7$  undergoes an antiferromagnetic (AFM) transition at  $T_N = 56$  K while remaining metallic, and then a Mott-like transition at  $T_{\text{MI}} = 48$  K [8–19] with a dramatic reduction (up to a factor of 20) in the conductivity for  $T < T_{\text{MI}}$  [8–12]. This transition is accompanied by an abrupt shortening of the  $c$ -axis lattice parameter below  $T_{\text{MI}}$  [10]. Such magnetoelastic coupling results in Jahn-Teller distortions of the  $\text{RuO}_6$  octahedra [9,10], thus lowering  $d_{xy}$  orbitals relative to  $d_{zx}$  and  $d_{yx}$  orbitals with a possible orbital distribution of  $(n_{xy}, n_{zx}/n_{yz}) = (2, 2)$  [18]. Consequently, an AFM and

OO phase can occur, explaining the poor metallic behavior for  $T < T_{MI}$  and  $B < B_c$  (critical field for the metamagnetic transition). This is consistent with Raman-scattering studies of  $\text{Ca}_3\text{Ru}_2\text{O}_7$  revealing that the transition at  $T_{MI}$  is associated with the opening of a charge gap,  $\Delta_c \sim 0.1$  eV, and the concomitant softening and broadening of an out-of-phase O phonon mode [13,14,18].

Single crystals were grown using both flux and floating zone techniques [20] and characterized by single crystal x-ray diffraction, Laue x-ray diffraction, scanning electron microscopy, and TEM. All results indicate that the single crystals are of high quality. The highly anisotropic magnetic properties of  $\text{Ca}_3\text{Ru}_2\text{O}_7$  are used to determine the magnetic easy  $a$  axis and to identify twinned crystals that often show a small kink at 48 K in the  $b$ -axis susceptibility.

Shown in Fig. 1 is the field dependence of the resistivity for the  $c$  axis (interplane)  $\rho_c$  (right scale) for  $T = 0.4$  K and  $0 \leq B \leq 45$  T with  $B \parallel a, b$ , and  $c$  axes.  $\rho_c$  is extraordinarily sensitive to the orientation of  $B$ . For the  $B \parallel a$  axis (magnetic easy axis),  $\rho_c$  shows an abrupt drop by an order of magnitude at 6 T, corresponding to the first-order metamagnetic transition leading to the spin-polarized or ferromagnetic (FM) state with a saturated moment  $M_s$  of  $1.8\mu_B/\text{Ru}$  or more than 85% polarized spins (see left scale in Fig. 1) [8,9]. The reduction of  $\rho_c$  is attributed to the coherent motion of electrons between Ru-O planes separated by insulating Ca-O planes, a situation similar to spin-filters where the probability of tunneling depends on the angle between the spin magnetization of adjacent ferromagnets. The fully spin-polarized state can lower the resistivity by at most a factor of 10. As  $B$  is increased further from 6 to 45 T,  $\rho_c$  increases linearly with  $B$  by more than 30%, which is interesting in its own right since a quadratic

dependence is expected for regular metals [21]. Because spin scattering is already reduced to its minimum at  $B = 6$  T, the linear increase can arise only from orbital degrees of freedom that via spin-orbit coupling hinder the electrons from hopping.

For the  $B \parallel b$  axis (magnetic hard axis), there is no spin-flop transition and the system remains AFM. In sharp contrast with  $\rho_c$  for the  $B \parallel a$  axis,  $\rho_c$  for the  $B \parallel b$  axis rapidly decreases by as much as 3 orders of magnitude at  $B_c = 15$  T, 2 orders of magnitude more than that for  $B \parallel a$ , where spins are fully polarized. For the  $B \parallel c$  axis, on the other hand,  $\rho_c$  displays Shubnikov-de Haas (SdH) oscillations with low frequencies of 28 and 10 T [22]. (The SdH effect reappears with vastly different behavior when  $B$  rotates within the  $ac$  plane [23].) Remarkably,  $\rho_c$  for  $B \parallel c > 39$  T is much smaller than  $\rho_c$  for  $B \parallel a$ . From 0 to 45 T,  $\rho_c$  decreases by a factor of 7 and 40 for  $B \parallel a$  and  $B \parallel c$ , respectively.

Since the fully polarized state for  $B \parallel a > 6$  T can reduce  $\rho$  by only 1 order of magnitude, so even the  $b$ -axis  $M$  were fully polarized at high fields, it still cannot account for the 3 orders of magnitude decrease in  $\rho_c$  when  $B \parallel b > 15$  T, indicating that the spin degree of freedom alone is not at all enough to explain the behavior observed in Fig. 1. It is striking that a fully spin-polarized state, which is essential for magnetoresistance in all other magnetoresistive materials [24,25], is the *least favorable* for conduction in  $\text{Ca}_3\text{Ru}_2\text{O}_7$ . It deserves mentioning that the resistivities  $\rho_a$  and  $\rho_c$  behave very similarly, as shown in the inset. For  $B \parallel a$ , the decrease in  $\rho_a$  is also 1 order of magnitude, the same as that of  $\rho_c$ , suggesting that the reduction in both  $\rho_a$  and  $\rho_c$  is driven by the same in-plane spin polarization. For  $B \parallel b$ ,  $\rho_a$  decreases by 2 orders of magnitude when

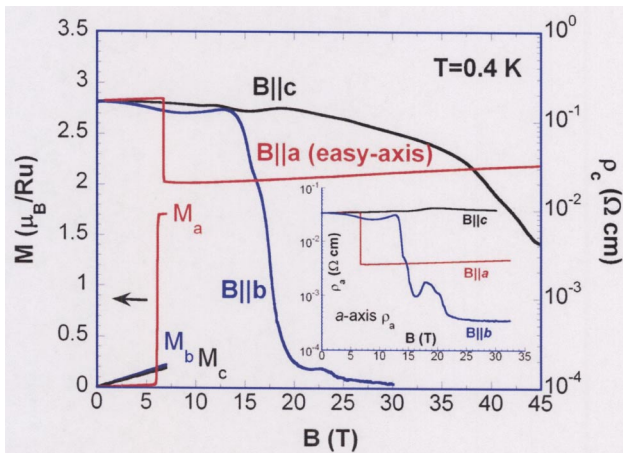


FIG. 1 (color online). Isothermal magnetization  $M$  for the  $B \parallel a, b$ , and  $c$  axes at  $T = 2$  K (left scale). Magnetic field dependence of the  $c$ -axis resistivity  $\rho_c$  for the  $B \parallel a, b$ , and  $c$  axes at  $T = 0.4$  K (right scale). Note that the magnetic easy axis is along the  $a$  axis with spin polarization of more than 85%. Inset:  $B$  dependence of the  $a$ -axis resistivity  $\rho_a$  for the  $B \parallel a, b$ , and  $c$  axes at  $T = 0.4$  K.

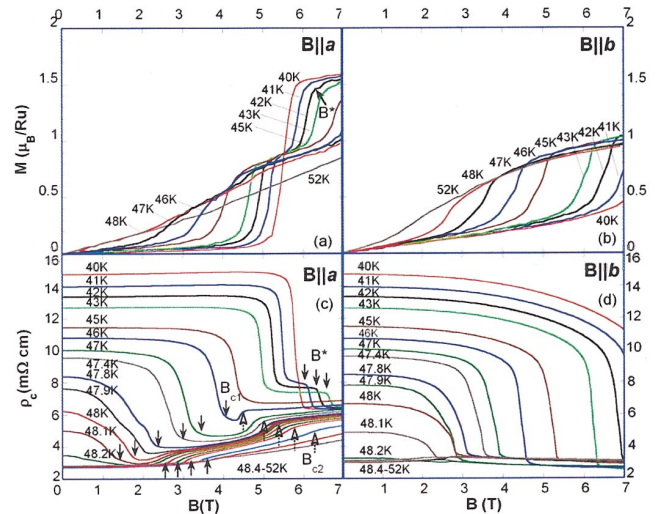


FIG. 2 (color).  $M$  and  $\rho_c$  as a function of  $B$  for the  $B \parallel a$  axis [panels (a) and (c)] and the  $b$  axis [panels (b) and (d)] for  $40 \leq T < 56$  K. The solid arrows (open arrows) indicate  $B^*$  or  $B_{c1}$  ( $B_{c2}$ ).

$B > B_c$ , confirming that the spin-polarized state is indeed not favorable for electron hopping. The striking behavior is that  $\rho_a$  ( $\sim 10^{-3} \Omega \text{ cm}$ ) is larger than  $\rho_c$  ( $\sim 10^{-4} \Omega \text{ cm}$ ) when  $B > B_c$ , although the opposite is true when  $B < B_c$ . There may be a change in effective dimensionality driven by  $B$  that results in incoherent-coherent and dimensional crossover and thus smaller interplane  $\rho_c$  when  $B > B_c$ . The crossover, if any, has a lesser impact on the intraplane  $\rho_a$ . This behavior driven by  $B$  could be analogous to that driven by temperature discussed in Ref. [26].

Shown in Fig. 2 are  $M$  and  $\rho_c$  as a function of  $B$  for the  $B \parallel a$  and  $b$  axes for  $40 \leq T < 56$  K. The advantage of this temperature range is that  $B_c$ , along both the  $a$  and the  $b$  axis, falls within the range of 7 T, so that  $M$  can be fully characterized using a SQUID magnetometer. A direct comparison of  $\rho$  and  $M$  allows to further probe correlations and the role of OO. Figure 2(a) displays  $M$  as a function of  $B$  for the  $B \parallel a$  axis. At 40 K,  $M(B)$  is still very similar to  $M(B)$  at low temperatures (see Fig. 1) but with slightly lower  $M_s$  ( $= 1.6 \mu_B/\text{Ru}$ ) and  $B_c$  ( $= 5.8$  T). For  $41 \leq T \leq 45$  K, a second transition develops at  $B^* > B_c$ , suggesting an intermediate FM state for  $B_c < B < B^*$ , which is not fully polarized along the  $a$  axis. A possible interpretation is that the spins are rotating away from the  $a$  axis due to a shortening of the  $c$  axis near  $T_{\text{MI}}$ , and hence a stronger field ( $B^*$ ) is required to realign these spins along the  $a$  axis. Since the spin rotation tends to become stronger as  $T$  approaches  $T_{\text{MI}}$ ,  $B^*$  increases with  $T$ .  $M$  is about  $1 \mu_B/\text{Ru}$  at  $B_c$  and increases by  $0.6 \mu_B/\text{Ru}$  at  $B^*$ . Only half of the ordered spins are thus aligned with the  $a$  axis in the spin reorientation (SR) region for  $B_c < B < B^*$ .  $B_c$  decreases with  $T$  and vanishes near  $T_N (= 56$  K). Unlike  $M$  for the  $B \parallel a$  axis,  $M$  for the  $B \parallel b$  axis is unsaturated at  $B > B_c$  and rounded at  $B_c$  without hysteresis, suggesting a second-order transition [see Fig. 2(b)]. Noticeably, the  $b$ -axis  $M$  at 7 T always converges to  $\sim 1 \mu_B/\text{Ru}$ , which is corresponding to 50% spin polarization and is independent of  $T$ . Clearly,  $M_s$  for the  $B \parallel b$  axis is always smaller than that for the  $B \parallel a$  axis in spite of the spin reorientation that partially enhances  $M$  for the  $B \parallel b$  axis.

The corresponding  $\rho_c$  as a function of  $B$  for the  $B \parallel a$  and  $b$  axes is displayed in Figs. 2(c) and 2(d), respectively. For the  $B \parallel a$  axis,  $\rho_c$  at 40 K shows an abrupt drop at  $B_c$  similar to that at low temperatures with a magnetoresistance ratio  $\Delta\rho/\rho(0) = 58\%$ , where  $\Delta\rho = \rho(7 \text{ T}) - \rho(0)$ . In the range  $41 \leq T \leq 45$  K,  $\rho_c$  for  $B \parallel a$  decreases initially at  $B_c$ , and then further at  $B^*$  with a total  $\Delta\rho/\rho(0)$  similar to that at 40 K. Clearly, for  $T \leq 45$  K,  $\rho_c$  perfectly mirrors the behavior of  $M$  for the  $B \parallel a$  axis, suggesting a strong spin-charge coupling in this region. However, for  $T \geq 46$  K, a valley develops in  $\rho_c$ ; the beginning and the end of this valley define two fields,  $B_{c1}$  ( $B_{c1} = B_c$  for  $T < 46$  K) and  $B_{c2}$ . The valley broadens with increasing  $T$  ( $B_{c1}$  decreases with  $T$ , while  $B_{c2}$  increases) and changes its shape for  $T \geq 48.2$  K, where the slope at  $B_{c1}$  is now

positive and  $B_{c1}$  increases with  $T$ . An important point is that the field dependence of  $\rho_c$  for  $46 \leq T \leq 52$  K does not track the field dependence of  $M$  [compare Figs. 2(a) and 2(c)]. This lack of parallel behavior of  $M$  and  $\rho_c$  is precisely a manifestation of the crucial role of the orbital degrees of freedom that dictate electron hopping for  $B \parallel a$ .

Furthermore, the reduction in  $\rho_c$  for the  $B \parallel b$  axis [Fig. 2(d)] is always much larger than that for the  $B \parallel a$  axis [Fig. 2(c)], and yet  $M_s$  for the  $B \parallel b$  axis is always smaller than  $M_s$  for the  $B \parallel a$  axis. For example, at 42 K and 7 T,  $\Delta\rho/\rho(0) = 50\%$  with  $M_s = 1.52 \mu_B/\text{Ru}$  for  $B \parallel a$ , and  $\Delta\rho/\rho(0) = 80\%$  with  $M_s = 1.03 \mu_B/\text{Ru}$  for  $B \parallel b$ . Note that the difference in both  $M_s$  and  $\Delta\rho/\rho(0)$  between the  $B \parallel a$  and  $b$  axes is  $\sim 35\%$ . The temperature dependence of  $M(7 \text{ T})$  (left scale) and  $\Delta\rho/\rho(0)$  at 7 T (right scale) for the  $B \parallel a$  and  $b$  axes is summarized in Fig. 3(a). Such an inverse correlation between  $M$  and  $\Delta\rho/\rho(0)$  suggests that the spin-polarized state is indeed detrimental to

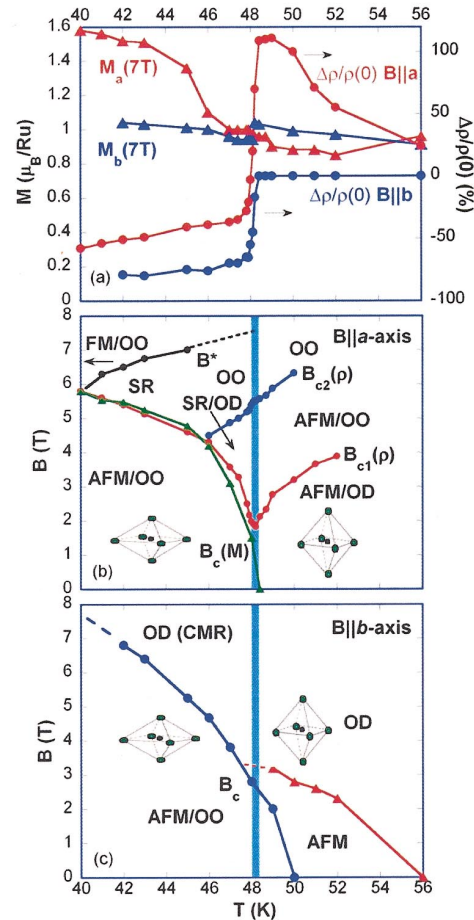


FIG. 3 (color). (a) Temperature dependence of  $M$  (triangles) and  $\Delta\rho/\rho(0)$  (solid circles, right scale) at 7 T for the  $B \parallel a$  and  $b$  axes. (b),(c) Phase diagrams plotted as  $B$  vs  $T$  summarizing various phases for the  $B \parallel a$  and  $b$  axes, respectively. Note that in (b)  $B_{c1}(\rho)$  and  $B_{c2}(\rho)$  indicate the curves generated based on  $\rho$ , and  $B_c(M)$  on  $M$ .

the CMR. For  $T > T_{MI}$ , the metallic state is recovered for  $B < B_{c1}$ . However, applying  $B$  along the  $a$  axis leads to a rapid increase in  $\rho_c$  with positive  $\Delta\rho/\rho(0)$  reaching as high as 112% for  $B > B_{c2}$ , whereas applying  $B$  along the  $b$  axis results in essentially no changes in  $\rho_c$ .

As is known, for  $B < 6$  T, the Mott-like state is due to the OO facilitated by the  $c$ -axis shortening at  $T_{MI}$  [12,18]. When  $B_{\parallel a} > 6$  T, the magnetic state becomes FM with the OO remained and stabilized by the FM state. The orbital order is either a ferro-orbital (FO) or an antiferro-orbital (AFO) configuration. Hence the system is in either a FM-FO or a FM-AFO state. The former inhibits the hopping of the  $4d$  electrons because of the Pauli exclusion principle, while the latter permits intersite transitions but at the expense of the Coulomb energy. Therefore, despite an order of magnitude drop in  $\rho_c$  due to the spin polarization when  $B > 6$  T, a fully metallic state can never be reached for the  $B \parallel a$  axis. In fact, the linear increase in  $\rho_c$  with increasing  $B$  for  $B_{\parallel a} > 6$  T, as shown in Fig. 1, may manifest a strengthened OO via the enhanced FM state. Conversely, applying  $B$  along the  $b$  axis steadily suppresses the AFM state [12], removing the orbital order through spin-orbit interaction when  $B > B_c$ . Such an orbitally disordered (OD) state drastically increases the electron mobility, therefore leading to CMR. On the other hand, applying  $B$  along the  $c$  axis has a noticeable impact on spin and orbital configurations when  $B > 35$  T where  $\rho_c$  drops rapidly and becomes much smaller than  $\rho_c$  for the  $B \parallel a$  axis. This suggests that the electronic state for the  $B \parallel a$  axis is the most resistive one.

The magnetic and transport behavior shown in Fig. 2 is remarkably consistent with rapid changes of the Ru-O phonon frequency with  $B$  seen in Raman studies [Fig. 2(b) in Ref. [18]], providing complementary evidence for the evolution of the field-induced magnetic and orbital phases. While applying  $B$  along the  $b$  axis clearly favors CMR, applying the  $B \parallel a$  axis generates a rich phase diagram [see Figs. 3(b) and 3(c)]. As shown in Fig. 3(b), below 40 K,  $B$  drives the system from an AFM-OO to a FM-OO state, and for  $40 < T < 48$  K the system enters a region of SR characterized by  $B_c$  and  $B^*$ . For  $46 \leq T < 48.2$  K, the valley seen only in  $\rho_c$  signals an onset of an OD state at  $B_{c1}$  and then a reoccurring OO state at  $B_{c2}$  characterized by a sharp increase in  $\rho_c$ . For  $48.2 < T < 56$  K, the system changes from an AFM-OD to an AFM-OO phase when  $B > B_{c1}$ . The evolution of the magnetic-orbital configuration is associated with the Jahn-Teller coupling, which appears in the vicinity of  $T_{MI}$ .

We have presented evidence that the orbital degree of freedom and its coupling to spin and lattice play a critical role in  $\text{Ca}_3\text{Ru}_2\text{O}_7$ . As a consequence, applying  $B$  along the  $a$ ,  $b$ , and  $c$  axes leads to novel and vastly different prop-

erties. Most notably, CMR achieved by avoiding the FM state is fundamentally different from that of all other magnetoresistive materials.

The authors thank Dr. L. Balicas for his help with measurements in the 45 T hybrid magnet at NHMFL. G.C. is grateful to Dr. S. Lance Cooper and Dr. Joseph Brill for their important comments on the Letter and to Dr. Ganpathy Murthy for very helpful discussions. This work was supported by NSF (Grant No. DMR-0240813). P.S. acknowledges the support by NSF (Grant No. DMR01-05431) and DOE (Grant No. DE-FG02-98ER45707).

---

\*Corresponding author.

Electronic address: cao@uky.edu

- [1] D.J. Singh and I.I. Mazin, Phys. Rev. B **63**, 165101 (2001).
- [2] T. Hotta and E. Dagotto, Phys. Rev. Lett. **88**, 017201 (2002).
- [3] V.I. Anisimov *et al.*, Eur. Phys. J. B **25**, 191 (2002).
- [4] A. Liebsch, Phys. Rev. Lett. **91**, 226401 (2003).
- [5] Z. Fang *et al.*, Phys. Rev. B **69**, 045116 (2004).
- [6] L. S. Lee *et al.*, Phys. Rev. Lett. **89**, 257402 (2002).
- [7] T. Mizokawa *et al.*, Phys. Rev. Lett. **87**, 077202 (2001).
- [8] G. Cao *et al.*, Phys. Rev. Lett. **78**, 1751 (1997).
- [9] G. Cao *et al.*, Phys. Rev. B **62**, 998 (2000).
- [10] G. Cao *et al.*, Phys. Rev. B **67**, 060406(R) (2003).
- [11] G. Cao *et al.*, Phys. Rev. B **67**, 184405 (2003).
- [12] G. Cao *et al.*, Phys. Rev. B **69**, 014404 (2004).
- [13] H. L. Liu *et al.*, Phys. Rev. B **60**, R6980 (1999).
- [14] C. S. Snow *et al.*, Phys. Rev. Lett. **89**, 226401 (2002).
- [15] A. V. Puchkov *et al.*, Phys. Rev. Lett. **81**, 2747 (1998).
- [16] R. P. Guertin *et al.*, Solid State Commun. **107**, 263 (1998).
- [17] S. McCall *et al.*, Phys. Rev. B **67**, 094427 (2003).
- [18] J. F. Karpus *et al.*, Phys. Rev. Lett. **93**, 167205 (2004).
- [19] E. Ohmichi *et al.*, Phys. Rev. B **70**, 104414 (2004).
- [20] There is *no difference* in the magnetic and transport properties and Raman spectra of crystals grown using flux and floating zone methods. Our studies on oxygen-rich  $\text{Ca}_3\text{Ru}_2\text{O}_{7+\delta}$  show that the resistivity for the basal plane shows a downturn below 30 K, indicating brief metallic behavior.
- [21] A. B. Pippard, *Magnetoresistance in Metals* (Cambridge University Press, Cambridge, 1989).
- [22] G. Cao *et al.*, New J. Phys. **6**, 159 (2004).
- [23] X. N. Lin *et al.* (unpublished).
- [24] For example, E. Y. Tsymbal and D. G. Pettifor, *Solid State Physics*, edited by Henry Ehrenreich and Frans Spaepen (Academic Press, New York, 2001), Vol. 56, p. 113.
- [25] For example, Yoshinori Tokura, *Colossal Magnetoresistive Oxides* (Gordon and Beach Science, Australia, 2000).
- [26] T. Valla *et al.*, Nature (London) **417**, 627 (2002).